Reactive Ni–Al-Based Materials

Energetic materials are substances or mixtures in which, under the action of external forces, self-sustaining chemical reactions occur with the release of a large amount of energy. A promising group of energetic materials are reactive structural materials (RSMs), consisting of two or more solids, usually nonexplosive metallic or nonmetallic powders, in which an exothermic reaction can occur after high-velocity impact and penetration into a target. As a rule, thermite, intermetallic, metal-fluoropolymer systems and metastable intermixed composites are used as RSMs.

1. Introduction

Energetic materials can be used in the military field as kinetic penetrators, cumulative highly reactive fragments, shaped charge liners [1], reactive projectiles, and reactive (active) armor and munition bodies [2][3][4]. RSMs must have mechanical properties comparable to traditional materials, such as steel, aluminum, copper, etc., which have a tensile strength of no less than 100 MPa. The most promising in terms of high strength are intermetallic systems. The compositions of Ni–Al, Al–W, Al–Zr, etc., in addition to high energy concentration, possess structural strength [1][5]. Since RSM components, as a rule, are powders, they must be consolidated. There are various technologies to consolidate RSMs into a monolithic structure: radial forging [2][6], cold and hot isostatic pressing [7][8], high-pressure torsion [9], magnetron sputtering [10] and cold spraying [11][12], cold rolling [13][14], accumulative roll-bonding [15], and explosive compacting [5][16]. The disadvantages of sputtering are its low rate and high cost. High-pressure processing requires large-sized equipment and includes multi-stage plastic deformation of two materials with different plasticity, which can eventually lead to material cracking and partial chemical interaction between starting components.

In addition to consolidation, there are methods for strengthening metallic [2][17], polymeric [18], and cement matrices [19], consisting of reinforcement with discrete [20] or continuous fibers. Data on the reinforcement of powder materials with ordered continuous fibers to increase their strength are not available in the literature.

At present, there is an increased interest in works aimed at identifying the basic laws of interaction between metals and polymer matrices composed of polytetrafluoroethylene (PTFE) during heating [21][22], shock-wave loading [23][24][25][26][27], and dynamic and static loading [28][29][30][31], with the variation in particle sizes [32]. The effect of sintering temperature on the strength of Al–PTFE compacts was investigated in [33]. In other works [34][35][36], an aluminum honeycomb was used to increase the energy release and strength of Al–PTFE compacts. The increased interest of researchers in the Al–PTFE mixture is primarily due to the ability of PTFE to form chemical compounds containing Al. The enthalpy of reaction for the mixture with a ratio of 26.5% Al/73.5% PTFE with the formation of AlF_3 was estimated as −8.85 kJ/g, considering the enthalpy of PTFE decomposition (8 kJ/g) and the enthalpy of AlF_3 formation (−18 kJ/g) [37]. The combustion heat per unit mass is 8.53 MJ/kg, which exceeds that of TNT more than twice [38]. In [39], it was found that the addition of PTFE reduces the critical initiation pressure in the Ni–Al intermetallic system.

Producing, testing, and studying promising RSMs with a certain set of physical and mechanical characteristics and high energy release are associated with several physical and chemical limitations and technological difficulties. Such studies, as a rule, are purely experimental and characterized by rapid physical and chemical processes, and high strain rates, pressures, and temperatures in reaction mixtures during explosive loading.

This paper presents studies of the strength, ignition, combustion, and shock-wave initiation of metal and metal-polymer powder mixtures based on Ni–Al and Ni–Al–PTFE. The effect of reinforcement with tungsten and boron fibers, low-temperature heat treatment (HT), and component fraction changes on the mechanical properties, phase formation, and energy characteristics of reactive powder compacts was investigated.

2. Strength and Combustion Behavior

The above-described procedure was used to prepare the specimens reinforced with continuous boron and tungsten fibers with powder matrices Ni–Al and Ni–Al–PTFE. Thermodynamic calculations were performed to select the stoichiometric composition of Ni–Al with the highest adiabatic combustion temperature (1638 °C). We found that the strength characteristics of the prepared specimens, namely the flexural strength of powder compacts with different molar ratios of nickel and aluminum (Ni–3Al, Ni–Al, and 3Ni–Al), are identical and lie in the range of 11 to 13 MPa at a relative density of 0.7. So, the choice of a Ni–Al stoichiometric composition is not only due to the high adiabatic combustion temperature, but also due to the strength.

For reinforced specimens, the optimal arrangement of fibers, which was determined experimentally, is of great importance. Laying one or two fibers did not provide a significant increase in strength. An excessive number of fibers reduces the strength characteristics of the material. The optimal number of fibers per layer for each fiber type is shown in Figure 6. Figure 7 shows the strength characteristics for different specimen types as a function of density. We found that increasing the density of compacts by 10% increased the strength of unreinforced specimens by 190%, with boron fibers by 170%, and with tungsten fibers by 65%. The boron fibers increased the strength by 60% and the tungsten fibers by 200% compared with unreinforced specimens. The reason for the increased strength of powder compacts is related to the redistribution of the load from the matrix to the fiber due to mechanical interlocking and friction between the powder and the fibers. It is necessary to note that there is a problem of insufficient adhesion of fiber with the matrix. This phenomenon mainly occurs with boron fibers. So, when bending, they are pulled out from the matrix without being destroyed, and as a result, are not possible to use to their full potential.
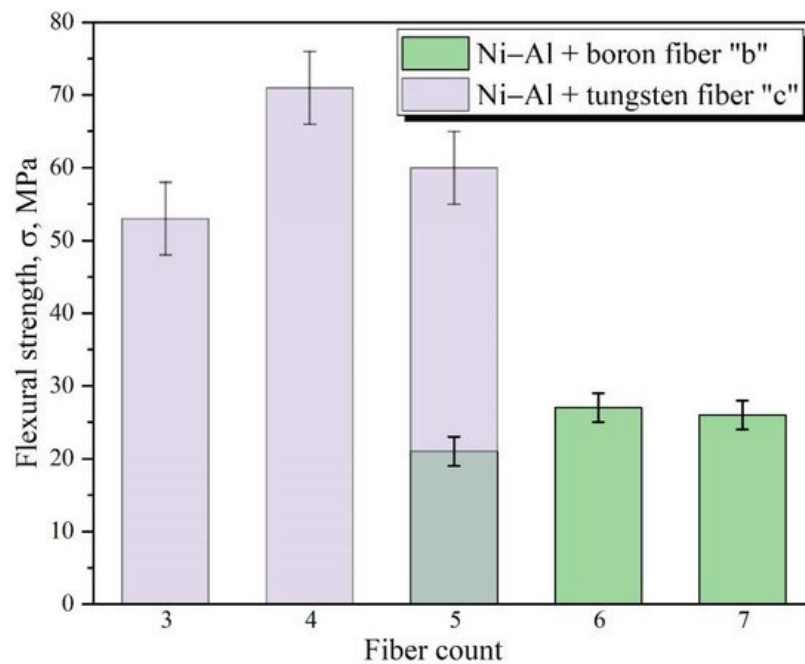

Figure 6. Flexural strength of specimens as a function of the number of fibers in one layer.
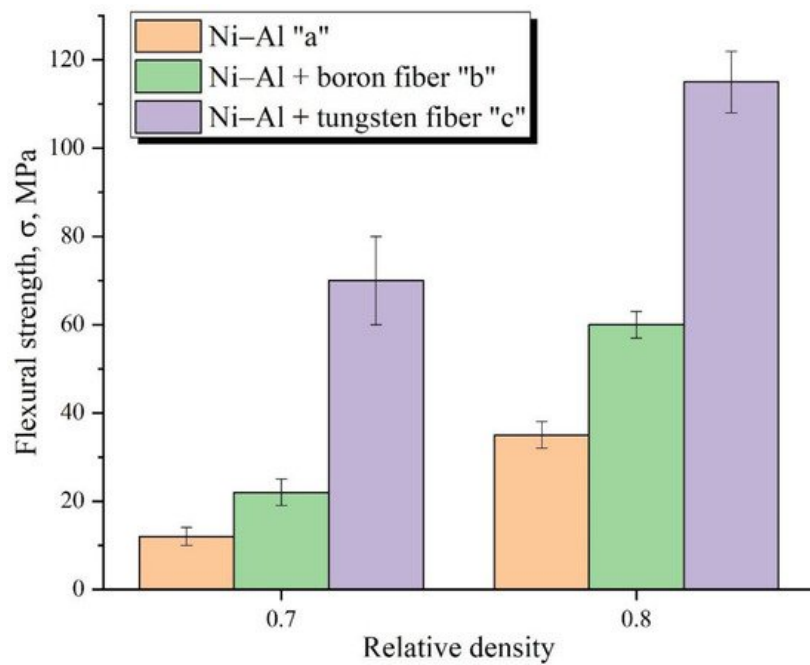
Figure 7. Flexural strength of specimens with different reinforcements.

The dependencies of flexural strength of the specimens on the type of reinforcement and HT modes are shown in Figure 8. HT of specimens in air provided a significant increase in flexural strength from 12 to 100 MPa for unreinforced specimens, but for specimens reinforced with boron fibers, it had no positive effect due to the weakening of the fibers [40].
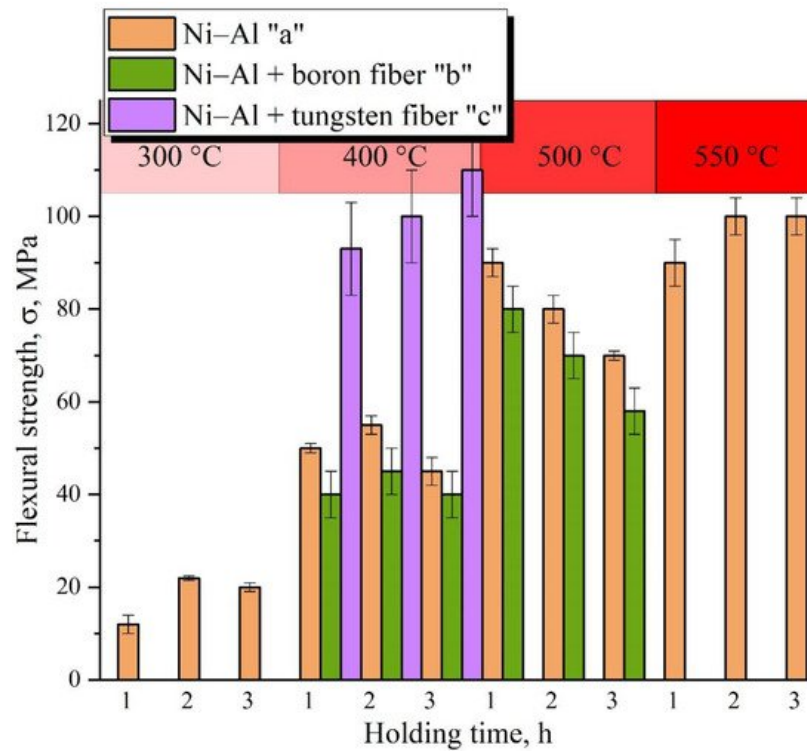

Figure 8. Flexural strength of specimens after HT.

HT of type a specimens increased their strength by 40% at 300 °C for 2 h, by 350% at 400 °C for 2 h, by 650% at 500 °C for 1 h, and by 730% at 550 °C for 2–3 h. Before HT, the type b specimens had an average strength of 23 MPa. The strength of the specimens increased by 90% at 400 °C for 2 h and by 250% at 500 °C for 2 h. The tungsten-fiber-reinforced specimens had an average strength of 60 MPa before HT, and after HT, the strength increased by 80% to 110 MPa at 400 °C for 3 h. HT of type a and c specimens provided hardening due to sintering of material, which is caused by the reduction in voids in the specimen, consequently resulting in denser and stronger material.

Specimens subjected to HT for 1 h at 400 and 500 °C contained NiO, and at 550 °C, in addition to the oxidation of nickel, a partial synthesis of the starting components with the formation of intermetallic compounds (Ni_2Al_3, $NiAl_3$) occurred, as seen in the X-ray diffraction patterns (Figure 9). A similar effect is observed for magnetron sputtering [10] and shockwave loading [5], which reduces the number of reactive components.
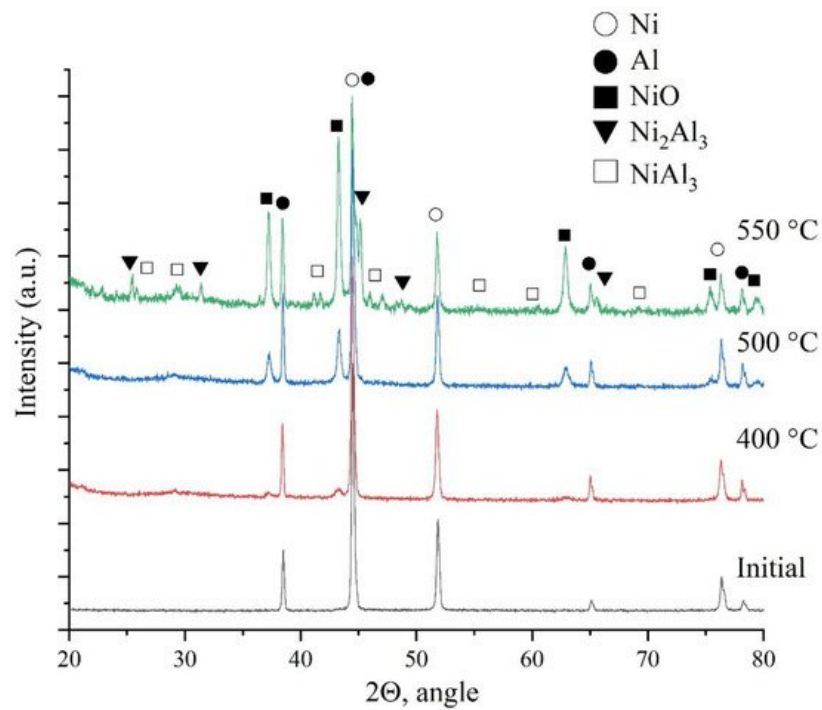
Figure 9. XRD of type a specimens before and after HT.

Figure 10 shows the dependence of strength of the powder Ni–Al–PTFE compacts on the proportion of PTFE and the type of reinforcement (relative density is provided for each specimen). The content of 1 wt % PTFE in the Ni–Al compact reinforced with boron fibers led to an increase in strength by 30% and to a decrease in strength by 30–35% for 3–5 wt % PTFE. Increasing the proportion of PTFE in the Ni–Al specimens increased the relative density, but it had a negative effect on their strength characteristics due to the low friction coefficient of PTFE.
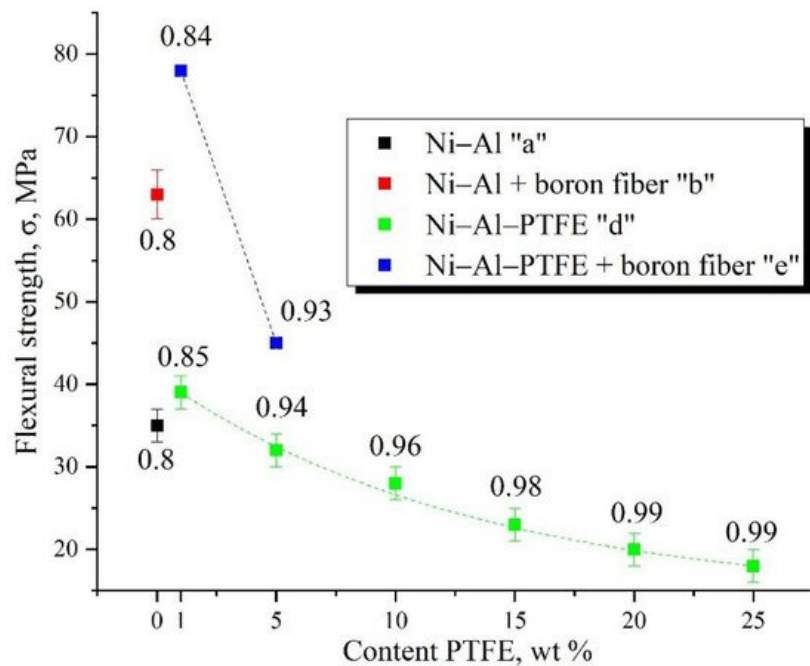

Figure 10. Flexural strength of Ni–Al–PTFE specimens.

Figure 11 shows the fracture of Ni–Al and Ni–Al–PTFE specimens with different types of reinforcement. The specimens of type a have a brittle and fast fracture. The specimens of type b fractured gradually along with pulling, bending, and breaking.
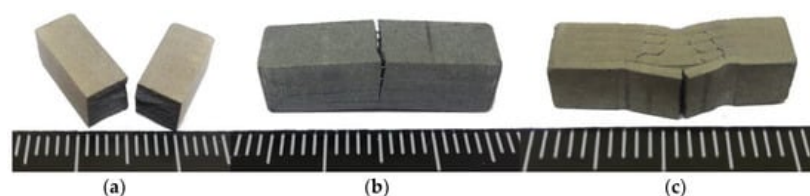
Figure 11. Specimens after bending tests: (**a**) without fibers, (**b**) with boron fibers, and (**c**) with tungsten fibers.

The investigation of the ignition of Ni–Al and Ni–Al–PTFE specimens before and after HT is shown in Figure 12 and Table 3, respectively. We found that the Ni–Al mixture ignited at about 660 °C, which corresponds to the melting temperature of Al and agrees with the results of DTA and DSC in the works [11][12][41][42]. After HT of the Ni–Al specimens, the ignition temperature increased from 660 to 980 °C, which is associated with the formation of oxide films on the surface of aluminum and nickel particles, preventing the aluminum from melting and spreading over nickel. In the Ni–Al–PTFE specimens, the ignition temperature was about 620–640 °C. According to the data of [41], at a heating rate of 10 °C/min, the reaction proceeded at 585 °C. In the present experiments, the recorded temperature was higher due to the high heating rate, as explained by the authors in [43]. The ignition temperature can be reduced using nanosized powders [44] or high-energy ball milling (HEBM) [10][45] and cryomixing [46]. The use of nanopowders is associated with difficulties such as agglomeration and autoignition in air. HEBM of powders leads to the synthesis of some starting components and reduces the formability of powder compacts as well.
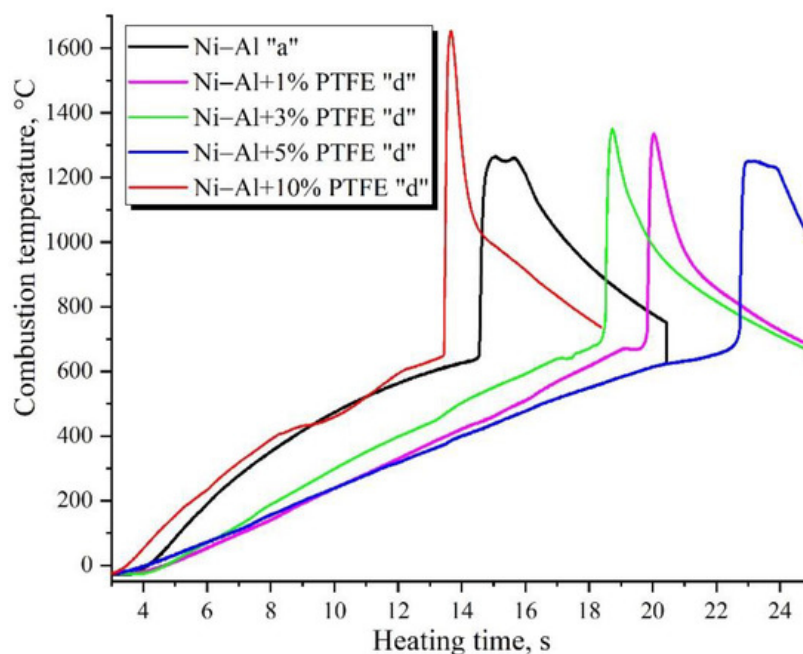

Figure 12. Thermograms of ignition of Ni–Al and Ni–Al–PTFE powder mixtures.

Table 3. Temperature of ignition of Ni–Al specimens after HT.

Combustion rate measurements showed that increasing the relative density of type a compacts from 0.7 to 0.8 led to an increase in the combustion rate by 25% (Figure 13). The addition of 1 wt % PTFE to the Ni–Al powder mixture led to an increase in the combustion rate from 35 to 120 mm/s, which is comparable to that of thin aluminum–fluoropolymer films studied in [47]. When the PTFE proportion increased from 15 to 25 wt %, the combustion rate decreased to 1.5 mm/s. This effect is associated with gas evolution in the combustion wavefront, which leads to the loosening of the specimen and interruption of heat exchange. Figure 14 shows the X-ray diffraction patterns of the burned Ni–Al–PTFE specimens. The only synthesis product is NiAl. During combustion, a large amount of gaseous products is formed, which are deposited on the reactor walls, but their presence in the specimens was not detected.
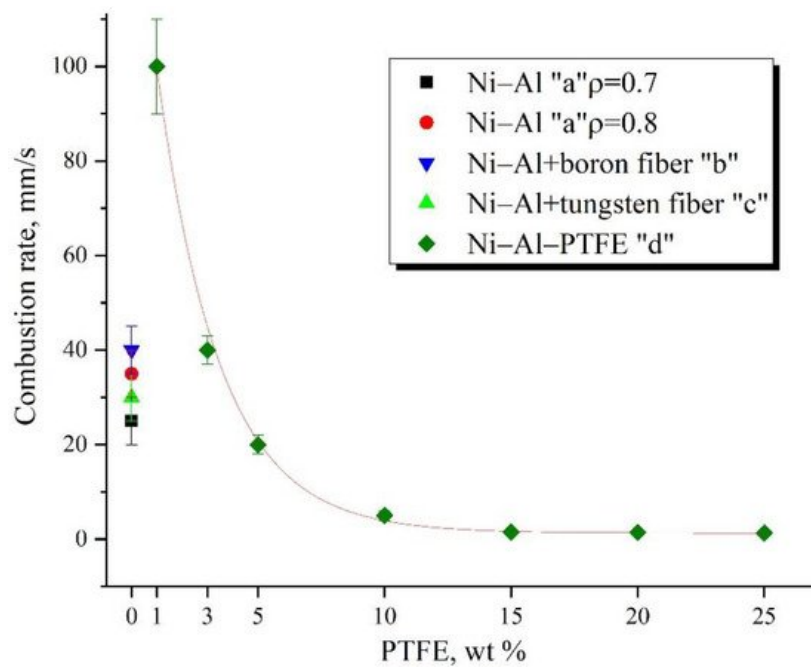
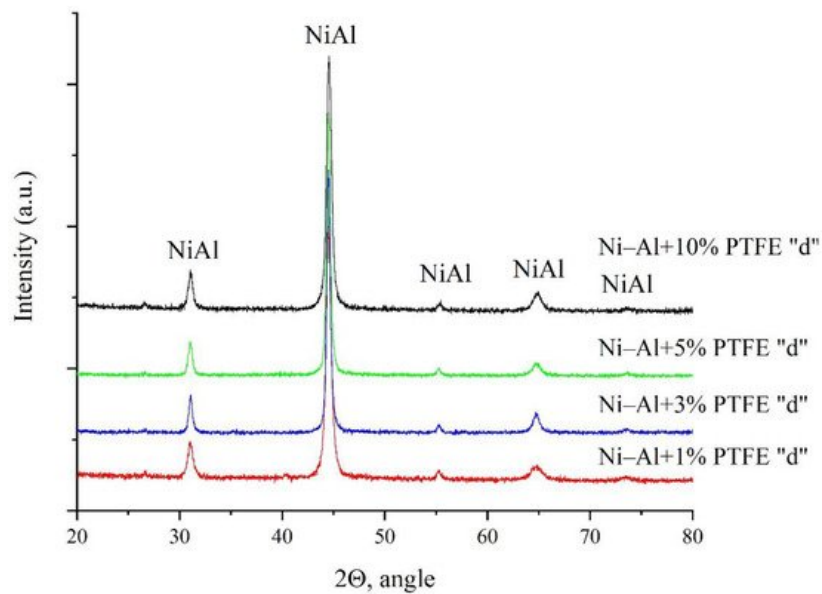**Figure 13.** Combustion rates for different types of specimens.

Figure 14. XRD of burned Ni–Al–PTFE specimens.

Figure 15 shows the video frames of combustion in the Ni–Al and Ni–Al–PTFE powder systems with different types of reinforcement. During the combustion of the Ni–Al specimens, there was no significant gas evolution or change in size, in contrast with specimens with the addition of fluoroplastic which significantly changed the initial size and mass. Combustion of the Ni–Al specimens with the introduction of boron fibers noticeably changed, demonstrating a rapid separation of hot particles from the surface of the sample. Combustion of Ni–Al with the addition of 1 and 3 wt % PTFE occurred with active heat release characterized by high temperature and high gasification of combustion products.

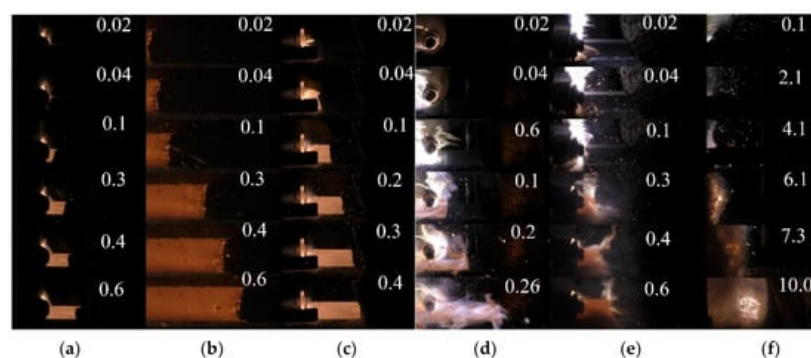**Figure 15.** Video frames of combustion in the Ni–Al system (time is given in seconds): (**a**) unreinforced; (**b**) with boron fibers; (**c**) with tungsten fibers; (**d**) with 1 wt % PTFE; (**e**) with 3 wt % PTFE; (**f**) with 15 wt % PTFE.

Synthesis in the Ni–Al and Ni–Al–PTFE systems subjected to shockwave loading was determined by visual inspection and XRD. Visual inspection revealed that shockwave loading of Ni–Al specimens, as well as with the addition of 1 and 3 wt % PTFE at throwing speeds of 1.0 and 1.5 km/s, did not result in combustion (Figure 16). At the throwing speed of 1.5 km/s, 5 wt % PTFE addition was sufficient to initiate the reaction (Figure 17), and at 1.0 km/s–10 wt % PTFE (Figure 16). Thus, the addition of PTFE lowers the threshold of initiation of shock waves in the Ni–Al system, positively affecting its reactivity.
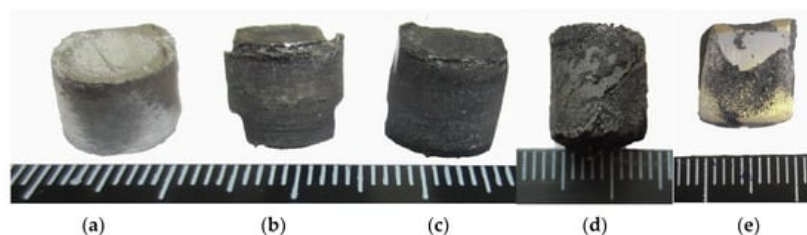

Figure 16. Specimens after shock-wave loading at 1 km/s: (**a**) Ni–Al; (**b**) with 1 wt % PTFE; (**c**) 5 wt % PTFE; (**d**) 10 wt % PTFE; (**e**) 15 wt % PTFE.
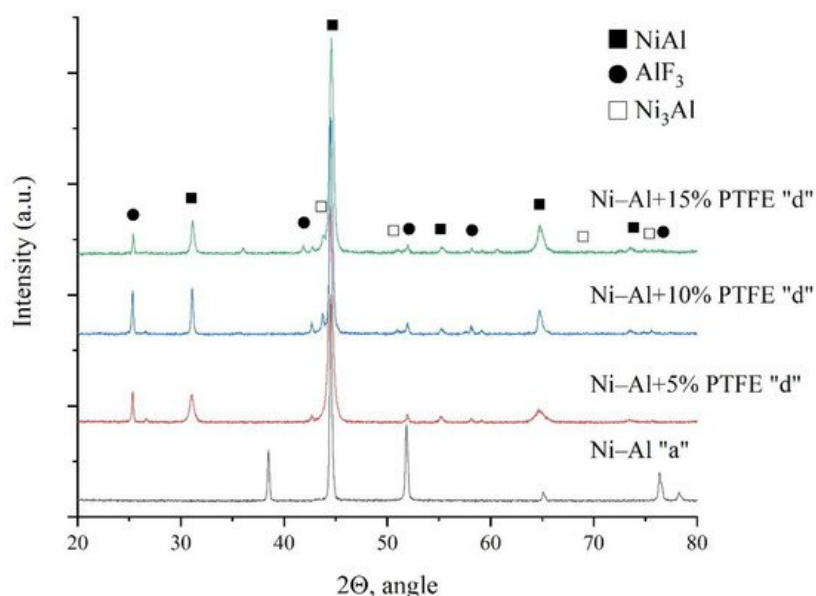

Figure 17. XRD of specimens after shock-wave loading at 1.5 km/s.

4. Conclusions

For the first time, the possibility of reinforcing reactive powder compacts with continuous fibers for increasing their strength characteristics was experimentally shown. The optimal schemes of reinforcement of RSM with boron and tungsten fibers, which increase the strength by 60% and 200%, were experimentally determined.

HT of Ni–Al at 400 °C and 550 °C for 3 h increased the ignition temperature to 740 °C and 980 °C, respectively. We found that HT of Ni–Al at temperatures of 400 and 500 °C for 1–3 h increases the strength by 650%, but it does not lead to chemical interaction between starting components. HT at 550 °C for 2–3 h increases the strength by 730%, but it leads to chemical interaction between starting components with the formation of $NiAl_3$ and Ni_2Al_3. The obtained results can be used to control the mechanical characteristics of reactive powder materials without reducing their reactivity. The strength of the specimens was 100–120 MPa, which is comparable to that of aluminum.

Adding PTFE up to 1 wt % to the Ni–Al specimens reinforced with boron fibers increases the strength by 27% by reducing porosity, but at more than 3 wt % PTFE decreases the strength by 30%. The addition of fluoroplastic to the Ni–Al specimens makes it possible to obtain materials with relative density up to 0.99 at relatively low pressures, which cannot be achieved without this addition.

We found that the addition of 5% and 10% PTFE to the Ni–Al system is sufficient to initiate an exothermic reaction at flyer plate velocities of 1.5 and 1.0 km/s.

References

1. Ren, H.; Liu, X.; Ning, J. Impact-initiated behavior and reaction mechanism of W/Zr composites with SHPB setup. AIP Adv. 2016, 6, 115205.

2. Hastings, D.L.; Dreizin, E.L. Reactive Structural Materials: Preparation and Characterization. Adv. Eng. Mater. 2017, 20, 1700631.

3. He, W.; Liu, P.-J.; He, G.-Q.; Gozin, M.; Yan, Q.-L. Highly Reactive Metastable Intermixed Composites (MICs): Preparation and Characterization. Adv. Mater. 2018, 30, 1706293.

4. Sun, M.; Li, C.; Zhang, X.; Hu, X.; Hu, X.; Liu, Y. Reactivity and Penetration Performance Ni–Al and Cu–Ni–Al Mixtures as Shaped Charge Liner Materials. Materials 2018, 11, 2267.

5. Zhou, Q.; Hu, Q.W.; Wang, B.; Zhou, B.B.; Chen, P.W.; Liu, R. Fabrication and characterization of the Ni–Al energetic structural material with high energy density and mechanical properties. J. Alloys Compd. 2020, 832, 154894.

6. Gibbins, J.D.; Stover, A.K.; Krywopusk, N.M.; Woll, K.; Weihs, T.P. Properties of reactive Al:Ni compacts fabricated by radial forging of elemental and alloy powders. Combust. Flame 2015, 162, 4408–4416.

7. Chiu, P.-H.; Olney, K.L.; Benson, D.J.; Braithwaite, C.; Collins, A.; Nesterenko, V.F. Dynamic fragmentation of Al–W granular rings with different mesostructures. J. Appl. Phys. 2017, 121, 045901.

8. Wang, M.; Li, J.; Zhang, J.; Liu, X.; Mao, Z.; Weng, Z.; Wang, H.; Tao, J. Microstructure Evolution and Compressive Properties of Multilayered Al/Ni Energetic Structural Materials under Different Strain Rates. J. Mater. Eng. Perform. 2020, 29, 506–514.

9. Renk, O.; Tkadletz, M.; Kostoglou, N.; Gunduz, I.E.; Fezzaa, K.; Sun, T.; Stark, A.; Doumanidis, C.C.; Eckert, J.; Pippan, R.; et al. Synthesis of bulk reactive Ni–Al composites using high pressure torsion. J. Alloys Compd. 2021, 857, 157503.

10. Baras, F.; Turlo, V.; Politano, O.; Vadchenko, S.G.; Rogachev, A.S.; Mukasyan, A.S. SHS in Ni/Al nanofoils: A review of experiments and molecular dynamics simulations. Adv. Eng. Mater. 2018, 20, 1800091.

11. Zhao, H.; Ning, X.; Tan, C.; Yu, X.; Nie, Z.; Sun, X.; Cui, Y.; Yang, Z.; Wang, F.; Cai, H. Influence of Al12Mg17 Additive on Performance of Cold-Sprayed Ni–Al Reactive Material. J. Therm. Spray Technol. 2019, 28, 780–793.

12. Yang, Z.; Ning, X.; Yu, X.; Tan, C.; Zhao, H.; Zhang, T.; Li, L.; Nie, Z.; Liu, Y. Energy Release Characteristics of Ni–Al–CuO Ternary Energetic Structural Material Processed by Cold Spraying. J. Therm. Spray Technol. 2020, 29, 1070–1081.

13. Miyake, S.; Izumi, T.; Yamamoto, R. Effect of the Particle Size of Al/Ni Multilayer Powder on the Exothermic Characterization. Materials 2020, 13, 4394.

14. Zhao, H.; Tan, C.; Yu, X.; Ning, X.; Nie, Z.; Cai, H.; Wang, F.; Cui, Y. Enhanced reactivity of Ni–Al reactive material formed by cold spraying combined with cold-pack rolling. J. Alloys Compd. 2018, 741, 883–894.

15. Wu, J.; Wang, H.; Fang, X.; Li, Y.; Mao, Y.; Yang, L.; Yin, Q.; Wu, S.; Yao, M.; Song, J. Investigation on shock-induced reaction characteristics of an Al/Ni composite processed via accumulative roll-bonding. Mater. Des. 2017, 116, 591–598.

16. Adamenko, N.A.; Kazurov, A.V.; Agafonova, G.V.; Savin, D.V. Structure Formation in Nickel-Polytetrafluorethylene Composite Materials upon Explosive Pressing of Powders. Inorg. Mater. Appl. Res. 2020, 11, 982–990.

17. Lin, C.; Han, Y.; Guo, C.; Chang, Y.; Han, X.; Lan, L.; Jiang, F. Synthesis and mechanical properties of novel Ti–(SiCf/Al3Ti) ceramic-fiber-reinforced metal-intermetallic-laminated (CFR-MIL) composites. J. Alloys Compd. 2017, 722, 427–437.

18. Ranjbar, N.; Zhang, M. Fiber-reinforced geopolymer composites: A review. Cem. Concr. Compos. 2020, 107, 103498.

19. Abdallah, S.; Fan, M.; Rees, D.W.A. Bonding Mechanisms and Strength of Steel Fiber–Reinforced Cementitious Composites: Overview. J. Mater. Civ. Eng. 2018, 30, 04018001.

20. Tang, E.; Li, S.; Chen, C.; Han, Y. Dynamic compressive behavior of fiber reinforced Al/PTFE active materials. J. Mater. Res. Technol. 2020, 9, 8391–8400.

21. Xiao, J.; Nie, Z.; Wang, Z.; Du, Y.; Tang, E. Energy release behavior of Al/PTFE reactive materials powder in a closed chamber. J. Appl. Phys. 2020, 127, 165106.

22. Chen, C.; Gao, R.; Guo, K.; He, L.; Chang, M.; Han, Y.; Tang, E. Thermoelectric behavior of Al/PTFE reactive materials induced by temperature gradient. Int. Commun. Heat Mass Transfer. 2021, 123, 105203.

23. Tolkachev, V.F.; Ivanova, O.V.; Zelepugin, S.A. Initiation and development of exothermic reactions during solid-phase synthesis under explosive loading. Therm. Sci. 2019, 23, 505–511.

24. Zelepugin, S.A.; Ivanova, O.V.; Yunoshev, A.S.; Zelepugin, A.S. Problems of Solid-Phase Synthesis in Cylindrical Ampoules under Explosive Loading. IOP Conf. Series: Mater. Sci. Eng. 2016, 127, 012057.

25. Ge, C.; Dong, Y.X.; Maimaitituersun, W.; Ren, Y.M.; Feng, S.S. Experimental study on impact-induced initiation thresholds of Polytetrafluoroethylene/Aluminum composite. Propellants Explos. Pyrotech. 2017, 42, 514–522.

26. Chen, C.; Tang, E.; Zhu, W.; Han, Y.; Gao, Q. Modified model of Al/PTFE projectile impact reaction energy release considering energy loss. Exp. Therm Fluid Sci. 2020, 116, 110132.

27. Jiang, C.; Cai, S.; Mao, L.; Wang, Z. Effect of Porosity on Dynamic Mechanical Properties and Impact Response Characteristics of High Aluminum Content PTFE/Al Energetic Materials. Materials 2020, 13, 140.

28. Ge, C.; Yu, Q.; Zhang, H.; Qu, Z.; Wang, H.; Zheng, Y. On dynamic response and fracture-induced initiation characteristics of aluminum particle filled PTFE reactive material using hat-shaped specimens. Mater. Des. 2020, 188, 108472.

29. Ren, H.; Li, W.; Ning, J. Effect of temperature on the impact ignition behavior of the aluminum/polytetrafluoroethylene reactive material under multiple pulse loading. Mater. Des. 2020, 189, 108522.

30. Feng, B.; Fang, X.; Li, Y.C.; Wang, H.X.; Mao, Y.M.; Wu, S.Z. An Initiation Phenomenon of Al–PTFE under Quasi-Static Compression. Chem. Phys. Lett. 2015, 637, 38–41.

31. Ge, C.; Dong, Y.; Maimaitituersun, W. Microscale Simulation on Mechanical Properties of Al/PTFE Composite Based on Real Microstructures. Materials 2016, 9, 590.

32. Wu, J.-X.; Fang, X.; Gao, Z.-R.; Wang, H.-X.; Huang, J.-Y.; Wu, S.-Z.; Li, Y.-C. Investigation on Mechanical Properties and Reaction Characteristics of Al–PTFE Composites with Different Al Particle Size. Adv. Mater. Sci. Eng. 2018, 2018, 1–10.

33. Wang, H.F.; Geng, B.Q.; Guo, H.G.; Zheng, Y.F.; Yu, Q.B.; Ge, C. The effect of sintering and cooling process on geometry distortion and mechanical properties transition of PTFE/Al reactive materials. Def. Technol. 2020, 16, 720–730.

34. Tang, E.; Luo, H.; Han, Y.; Chen, C.; Chang, M.; Guo, K.; He, L. Experimental study on burning of two Al/PTFE samples. Appl. Therm. Eng. 2020, 180, 115857.

35. Tang, E.; He, Z.; Chen, C.; Han, Y. Characterization of dynamic compressive strength and impact release energy of Al/PTFE energetic materials reinforced by aluminum honeycomb skeleton. Compos. Struct. 2020, 241, 112063.

36. He, Z.; Tang, E.; Ou, X.; Gao, X.; Jiang, L.; Chen, C.; Chang, M.; Han, Y. Energy release of Al/PTFE materials enhanced by aluminum honeycomb framework subjected to high speed impact under vacuum environment. Journal of Materials Research and Technology. J. Mater. Res. Technol. 2020, 9, 14528–14539.

37. Valluri, S.K.; Schoenitz, M.; Dreizin, E.L. Metal-rich aluminum–polytetrafluoroethylene reactive composite powders prepared by mechanical milling at different temperatures. J. Mater. Sci. 2017, 52, 7452–7465.

38. Chen, C.; Tang, E.; Luo, H.; Han, Y.; Duan, Z.; Chang, M.; Guo, K.; He, L. Heat conduction and deflagration behavior of Al/PTFE induced by thermal shock wave under temperature gradient. Int. Commun. Heat Mass Transf. 2020, 118, 104834.

39. Xiong, W.; Zhang, X.; Tan, M.; Liu, C.; Wu, X. The Energy Release Characteristics of Shock-Induced Chemical Reaction of Al/Ni Composites. J. Phys. Chem. C 2016, 120, 24551–24559.

40. Metcalfe, A. Interfaces in Metal Matrix Composites. In Composite Materials, 1st ed.; Metcalfe, A., Ed.; Academic Press: New York, NY, USA, 1974; Volume 1, pp. 64–126.

41. Wang, J.; Zeng, C.; Zhan, C.; Zhang, L. Tuning the reactivity and combustion characteristics of PTFE/Al through carbon nanotubes and grapheme. Thermochim. Acta 2019, 676, 276–281.

42. Ao, W.; Fan, Z.; Liu, L.; An, Y.; Ren, J.; Zhao, M.; Liu, P.; Li, L.K.B. Agglomeration and combustion characteristics of solid composite propellants containing aluminum-based alloys. Combust. Flame 2020, 220, 288–297.

43. Vadchenko, S.G.; Alymov, M.I.; Saikov, I.V. Ignition of Some Powder Mixtures of Metals with Teflon. Inorg. Mater. Appl. Res. 2018, 9, 517–522.

44. Turlo, V.; Politano, O.; Baras, F. Alloying propagation in nanometric Ni/Al multilayers: A molecular dynamics study. J. Appl. Phys. 2017, 121, 055304.

45. Beason, M.T.; Gunduz, I.E.; Son, S.F. The Role of Fracture in the Impact Initiation of Ni–Al Intermetallic Composite Reactives during Dynamic Loading. Acta Mater. 2017, 133, 247–257.

46. Oh, M.; Oh, M.C.; Han, D.; Jung, S.-H.; Ahn, B. Exothermic Reaction Kinetics in High Energy Density Al–Ni with Nanoscale Multilayers Synthesized by Cryomilling. Metals 2018, 8, 121.

47. Wang, H.; Rehwoldt, M.; Kline, D.J.; Wu, T.; Wang, P.; Zachariah, M.R. Comparison study of the ignition and combustion characteristics of directly-written Al/PVDF, Al/Viton and Al/THV composites. Combust. Flame 2019, 201, 181–186.